THE JOURNAL OF PHYSICAL CHEMISTRY B LETTERS

2006, *110,* 11607−11610
Published on Web 06/01/2006

Ordered Patterning of Nanometric Rings of Single Molecule Magnets on Polymers by Lithographic Control of Demixing

Massimiliano Cavallini,*,† Jordi Gomez-Segura,‡ Cristiano Albonetti,† Daniel Ruiz-Molina,‡ Jaume Veciana,‡ and Fabio Biscarini*,†

CNR-Istituto per lo Studio dei Materiali Nanostrutturati, Via P. Gobetti 101, I-40129 Bologna, Italy, and CSIC-Institut de Ciencia de Materials de Barcelona, Campus Universitari de Bellaterra, 08193 Cerdanyola, Spain

Received: February 27, 2006; In Final Form: April 28, 2006

We report a new patterning process which takes place as a result of demixing of a binary polymer/solute mixture. An efficient, sustainable approach for ordering nanosized rings of so-called single molecule magnets (SMMs) is thus provided. It exploits the self-organization process in which SMM patterned film evolves to a spatially correlated pattern of nanosized rings. At long time, the anisotropic patterning of the film drives the ring to coalesce, into parallel lines of nanometric width.

The demixing of binary polymer/polymer or in general polymer/solute mixtures at surfaces has been studied extensively during the past decades, and several applications of demixing have been proposed.[1] Among these, the fabrication of patterned thin films of single molecule magnets (SMMs)[2] by demixing has been recently reported.[3] The presence of a surface strongly influences the demixing process of the multicomponent blend, viz., polymer and solute.[4] Demixing leads to surface-oriented phase separation, were of a double layer consisting of the polymer and the solute is formed. The driving force of the demixing depends on the lower surface energy of the solute.[5] The thickness of the layers is determined by the volume ratio of the two phases in the initial blend. When a component of the blend is considerably lesser in percentage, it forms a thin film on the surface of the polymer matrix. Its spreading coefficient, S, can be defined as $S = \gamma_{PA} - \gamma_{SP} - \gamma$, where γ_{PA} is the surface tension of polymer/air, γ_{SP} is the surface tension of solute/polymer, and γ is the surface tension of solute/air. When S is negative, the thin film is thermodynamically unstable, leading to the fragmentation into smaller aggregates (droplets) in order to achieve the equilibrium conditions.[6] The thin film rupture results in the dewetting of segregated material from the polymer surface.

The two components used in this work are $Mn_{12}O_{12}(O_2CC_{12}H_9)_{16}(H_2O)_4$, (Mn12),[7] dispersed into commercial polycarbonate (PC). Mn12 is a convenient prototype single molecule magnet with potential impact in long term applications such as ultrahigh density magnetic storage,[8] quantum computing applications,[9] biosensors,[10] patterning by microcontact printing,[11] and nanopatterning by dewetting.[12] When dispersed in PC, it spontaneously forms a double layer by demixing upon solvent treatment.[13]

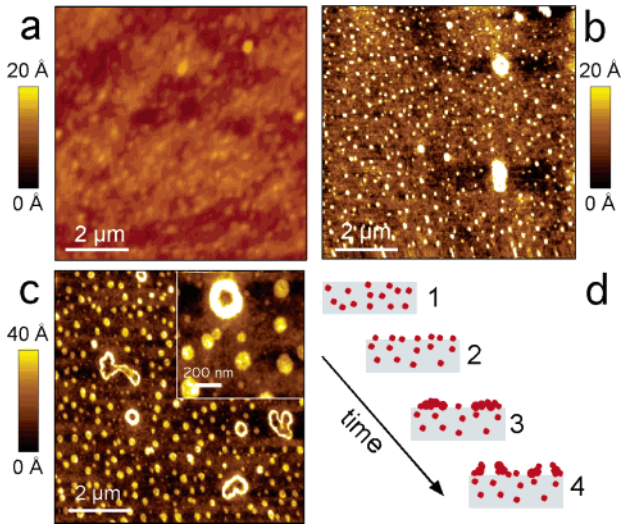

Figure 1. Evolution of the surface morphology of a Mn12/PC mixture film prepared by drop casting: (a) film after preparation; (b) film after 2 min of solvent exposure (the solute emerges to the surface); (c) film after 3 min of solvent exposure (the droplet reaches a critical diameter, forming the rings which then coalesce; the inset shows a ring 180 nm diameter); (d) scheme of the process (d1, film as prepared; d2, demixing; d3, droplet formation; d4, nanoring formation).

PC in pellets with Mn12 clusters (4% in weight) is dissolved in dichloromethane (CH_2Cl_2), and 50 μL of the solution is drop cast onto a glass surface. A smooth film 10 μm thick (measured by the α-step) is formed. After that, the film is exposed to a saturated atmosphere of CH_2Cl_2 vapors at room temperature, to induce the demixing of solute.

Figure 1 shows the morphological evolution of the sample upon solvent treatment and the scheme of the process. Before the solvent exposure, the surface of the cast film is very flat with a topographic root mean square (rms) roughness less than

* To whom correspondence should be addressed. Present address: CNR-ISMN, "Nanotechnology of Multifunctional Materials Research Division", Via P. Gobetti 101, I-40129 Bologna, Italy. Phone: +390516398519. Fax. +390516398539. E-mail: m.cavallini@bo.ismn.cnr.it (M.C.); f.biscarini@bo.ismn.cnr.it (F.B.).

† CNR-Istituto per lo Studio dei Materiali Nanostrutturati.

‡ CSIC-Institut de Ciencia de Materials de Barcelona.

10.1021/jp061231g CCC: $33.50

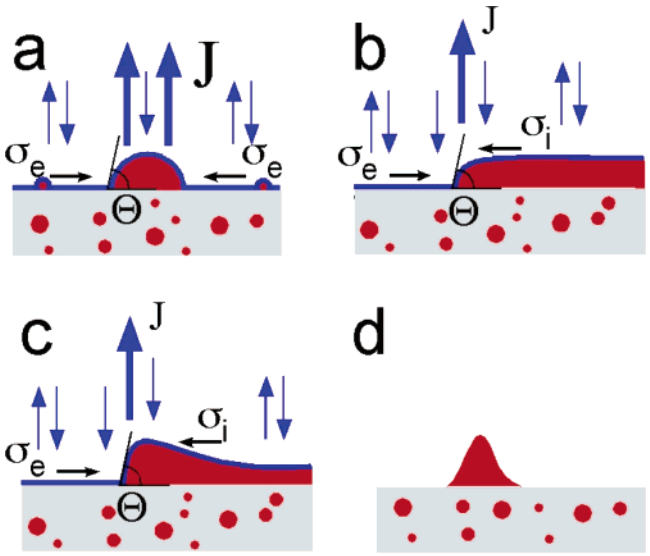

Figure 2. Schematic representation of droplet growth and its transformation in a nanoring (see description in the text).

1 nm (Figure 1a). The solvent exposure swells the film and solvates the polymer chains, decreasing the glass transition temperature of PC below room temperature. This exposure leads to the emergence of a fraction of the Mn12 molecules to the surface with the formation of nanometric droplets. This process can be controlled by the temperature, the partial pressure, and the nature of the solvent.[13]

During the solvent treatment, the topographic roughness increases from <1 to ~2 nm (Figure 1b). Due to thermodynamic instability, the emerging molecules, instead of forming a continuous film, dewet and give rise to a pattern of small aggregates in the form of droplets. These grow and coalesce during the solvent treatment, forming larger droplets. Upon a longer solvent treatment, when the droplets reach a critical diameter of about 100 nm, they transform into circular rings (Figure 1c). Eventually, the rings coalesce with each other, forming larger rings with irregular shape. It is remarkable that by interrupting the exposure to the solvent the transformation is stopped and the morphology remains frozen in the metastable form. Figure 1d shows the complete scheme of the process.

The transformation from droplets to rings has been observed in a variety of systems and at different length scales: InAs islands (dots ~50 nm diameter) grown on GaAs substrate,[14,15] blend containing nitrocellulose and $CoPt_3$ particles[2] (islands ~1 μm diameter), and a stain of coffee at the macroscopic scale.[16,17] Although the phenomenon is general, a conclusive model of the transformation of the droplets into rings has not been developed yet. Several phenomenological models have been proposed to explain the ring formation,[4,17] also using Monte Carlo simulations.[18]

Figure 2 shows a possible mechanism of this transformation. When the film of Mn12 clusters emerged to the surface is exposed to a solvent-saturated atmosphere, a thin layer of the solvent, which is in equilibrium with its vapors, condenses on the surface. In correspondence to the droplet edges, due to the higher Laplace pressure,[19] which depends on the higher curvature of the droplet, the solvent tends to evaporate faster.[16] This different evaporation rate induces a solvent flux (σ_e) that carries solute to the droplet (Figure 2a) where it concentrates and eventually precipitates. The small droplets, which have higher curvature, act as sites of nucleation which grow by adsorption of the material flowing from the outer parts of the surface. As the droplet grows, it reduces its curvature in the center (and hence the Laplace pressure) and reaches a critical diameter, where the evaporation rate in the center reduces (Figure 2b) with respect to the boundaries. On the other hand, the droplet boundaries are forced to maintain the contact angle (Θ) constant,[16] and hence the Laplace pressure and the associated higher evaporation rate. When the differential evaporation rate between the center and the boundaries of the droplet becomes relevant, an outward capillary flow (σ_i) compensates the amount of evaporated liquid. This flux transports soluble material and accumulates it to the droplet boundaries (Figure 2c) where it reaches supersaturation and reprecipitates. At the end of the process, the droplet transforms itself into the ring (Figure 2d). The rings can appear as nanometer cavities (pores) on the surface.

On the basis of this process, we used a patterned film of Mn12 on PC, to confine the ring formation inside the patterned regions.

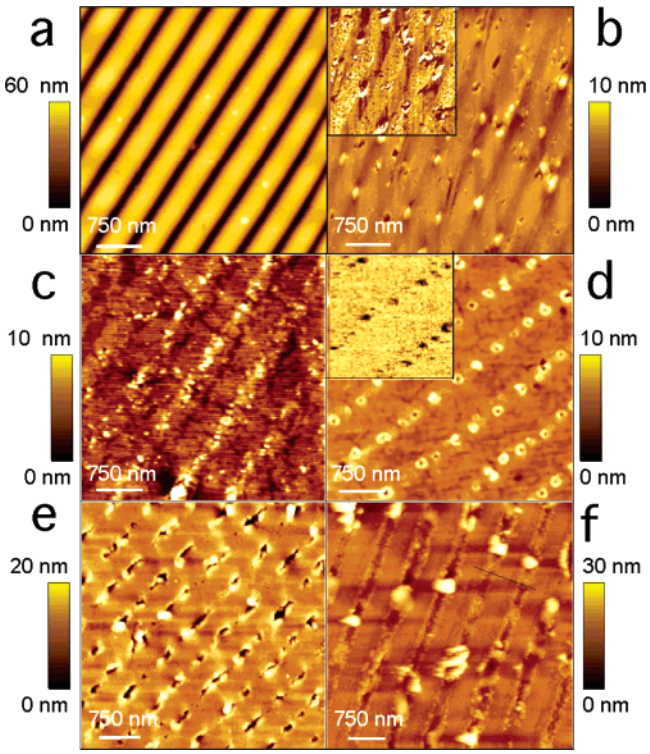

Figure 3. Morphological evolution of printed lines upon solvent treatment. (a) AFM topography image of a molded film of Mn12/PC, the ruler is 740 nm (topographic pattern). (b) After 2 min of solvent vapor treatment. The height of the protrusions has decreased by more than 96% compared to its 125 nm original value. The inset shows the corresponding phase contrast image where the inhomogeneous distribution of the Mn12 solute at the surface (chemical pattern) is resolved. The darker regions are depleted of the solute. (c) The film evolves to droplets by dewetting. (d) Upon longer solvent vapor treatment, the droplets transform into nanorings. The corresponding phase image (inset) shows that the inner part of the nanorings have different composition. (e) Upon longer solvent exposure, the nanorings evolve to an elongated shape. (f) Eventually, the nanorings coalesce, forming a single ring that looks like parallel lines 50 nm wide.

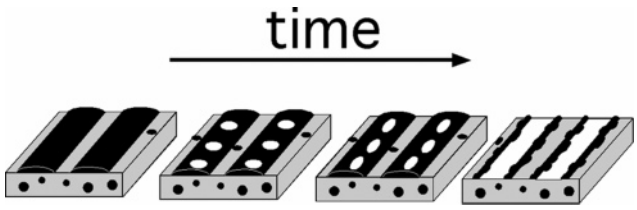

Figure 4. Scheme of the transformation of isolated nanorings to continuous parallel nanostripes.

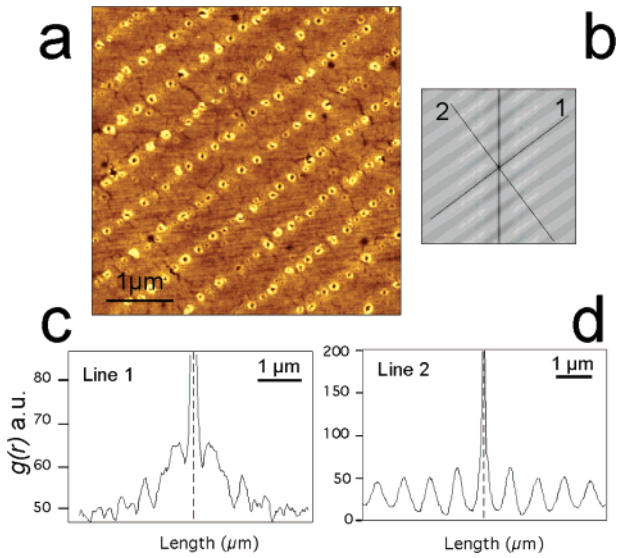

Figure 5. (a) AFM image of the early stage of ring formation. (b) 2D height−height correlation function ($g(r)$) of a. (c) Line profile of $g(r)$ measured along the stripe direction 1b. (d) Line profile of $g(r)$ measured perpendicularly to the stripe direction 2b.

The chemically patterned films[3] are prepared starting from molded Mn12/PC films that can be fabricated by several methods.[20,21] Here, the molded films are prepared by casting a solution of Mn12 and PC in CH_2Cl_2 onto a replica of a blank digital video disk (DVD) support that acts as a structured master. Once the solvent evaporates, the replica is removed from the master, resulting in a stable, flexible film (10 μm thick) of a solid solution of Mn12 in PC. The film surface, imaged by atomic force microscopy (AFM) in intermittent-contact mode (Figure 3a), exhibits an inverted pattern with respect to the DVD master, with parallel lines that are 300 nm wide and 125 nm deep and a periodicity between grooves of 740 nm. On a second step, the film is exposed to a saturated atmosphere of CH_2Cl_2 vapors at room temperature. The film swells and the glass transition temperature of the polymer is decreased below room temperature due to the solvation of polymer chains. Upon these conditions, the structured film surface experiences a smoothening driven by the minimization of the surface tension, which leads to the progressive deletion of the topographic relieves. The surface smoothening occurs at the same time as the demixing; thus, due to higher surface contraction in correspondence with the protrusions, the emerged molecules concentrate in these zones, transforming the topographic pattern into a chemical pattern (Figure 3b). The time scale for a complete smoothening depends on the experimental parameters, such as solvent nature, temperature, and initial surface roughness. Normally, a few minutes are sufficient to complete the process. AFM images of the molded replica after exposure to CH_2Cl_2 vapors for 2 and 3 min are shown in Figure 3b and c. The protrusions decrease by about 95% (rms roughness 56 nm → 3 nm) after 2 min of solvent exposure and by more than 99% (rms roughness <1 nm) after 3 min. As shown in the inset of Figure 3b, AFM phase contrast images show that the Mn12 clusters concentrate preferentially in the regions where the protrusions were originally formed, while they are almost absent from the grooves. After 3 min of solvent treatment, the sample results in a patterned film that is 3.5 ± 0.8 nm thick, which corresponds to two to three layers of molecules.[12]

The nanorings form and coalesce upon longer exposure to the solvent vapors (Figures 3d and 5a). The contrast observed in the corresponding phase image (see the inset of Figure 3d) suggests that the inner part of the rings has a different composition with respect to the boundaries. Since the emerging material is anisotropically distributed, the rings are forced to grow and to coalesce following the same anisotropy of the printed stripes. As a consequence, the rings assume an elongated shape (Figure 3e) and eventually after longer solvent treatment they form a single ring, which appears as two parallel lines (Figure 3f). The scheme of the process is depicted in Figure 4.

Although occasionally was observed a random distribution of the rings inside the lines, usually they result in being spatially correlated. Figure 5 evidences an AFM image on a larger scale and the statistical analysis of pore distribution at the early stages of their formation (i.e., corresponding to Figure 3d). The 2D fast Fourier transformation of the images shows the periodicity of the printed lines. This is confirmed by the height−height correlation function ($g(r)$) (Figure 5c). The $g(r)$ measured along line 1 (Figure 5c corresponding to stripe direction) shows peaks as a consequence of strong spatial correlations among the rings, which extend up to the third neighbor (Figure 5c).

In summary, we present an application of the demixing process combined with chemical patterning of a binary polymer/solute mixture for the fabrication.

In our work, we demonstrate how a Mn12 patterned film spontaneously evolves in a spatially correlated pattern of nanorings and how this process is controlled for nanopatterning.

This process is sustainable, since it does not require special tools or instrumentation. It is versatile and reproducible, and makes it possible to fabricate an ordered pattern of nanometric rings in a straightforward manner. Here, we used Mn12 clusters as representative material, but in principle, the approach can be extended to other soluble molecular materials and polymers, demixing upon solvent treatment or thermal annealing.

Experimental Section

Samples Preparation. Poly(bisphenol A carbonate) (PC) (Aldrich) in pellets with $Mn_{12}O_{12}(O_2CC_{12}H_9)_{16}(H_2O)_4$ [7] SMM (4% in weight) is dissolved in 10 mL of CH_2Cl_2 (Aldrich spectroscopic grade quality). The solution is cast on a master blank digital video disk (DVD) previously covered with a 100 nm thick Au film.

The molded films are prepared by casting 50 μL of Mn12 and PC in CH_2Cl_2 onto a replica of the structured master. Once the solvent is evaporated, the replica is removed from the master, resulting in a stable, flexible film (10 μm thick) of a solid solution of Mn12 in PC. The sample thickness was measured by a commercial α-step. Circular samples of a 1 cm diameter were fabricated.

Atomic Force Microscopy. AFM images were recorded with a standalone atomic force microscope (SMENA NT-MDT Moscow) operated in air in intermittent-contact mode (25 °C with a relative humidity of 55%). Silicon cantilevers (NT-MDT NSG10, with the typical curvature radius of the tip being 10 nm and the typical resonant frequency being 255 kHz) were used. All images are unfiltered. The topographic images were corrected line by line for background trend by removal of the second-order polynomial fitting. Image analysis was carried out ex situ with the image analysis software IMAGE-SXM 1.75, and analyses of the autocorrelation spectra along the directions parallel and perpendicular to the printed features were carried out with Igor Pro 4.0.

Acknowledgment. This work was partly supported by EU NAIMO Integrated Project No. NMP4-CT-2004-500355 and ESF-SONS project FUNSMARTS. We would like to thank Jean Francois Moulin, Rajendra Kshirsagar, and Massimiliano Massi

for stimulating discussions and suggestions and Emilia Arisi for her help.

References and Notes

(1) Walheim, S.; Boltau, M.; Mlynek, J.; Krausch G.; Steiner, U. *Macromolecules* **1997**, *30*, 4995

(2) Sessoli, R.; Gatteschi, D.; Caneschi, A.; Novak, M. A. *Nature* **1993**, *365*, 141.

(3) Cavallini, M.; Gomez-Segura, J.; Ruiz-Molina, D.; Massi, M.; Albonetti, C.; Rovira, C.; Veciana, J.; Biscarini, F. *Angew. Chem., Int. Ed.* **2005**, *44*, 888.

(4) Govor, L. V.; Reiter, G.; H. Bauer, G.; Parisi J. *Appl. Phys. Lett.* **2004**, *84*, 4774.

(5) Bruder, F.; Brenn, R. *Phys. Rev. Lett.* **1992**, *69*, 624.

(6) Brochard-Wyart F.; Daillant J. *Can. J. Phys.* **1990**, *68*, 1084.

(7) Ruiz-Molina, D.; Gerbier, P.; Rumberger, E.; Amabilino, D. B.; Guzei, I. A.; Folting, K.; Huffman, J. C.; Rheingold, A. L.; Christou, G.; Veciana, J.; Hendrickson, D. N. *J. Mater. Chem.* **2002**, *12*, 1152.

(8) Awschalom, D. D.; Kikkawa J. M. *Phys. Today* **1999**, *52*, 33.

(9) Ohno, H.; Chiba, D.; Matsukura, F.; Omiya, T.; Abe, E.; Dietl, T.; Ohno, Y.; Ohtani, K. *Nature* **2000**, *408*, 944.

(10) Edelstein, R. L.; Tamanaha, C. R.; Sheehan, P. E.; Miller, M. M.; Baselt, D. R.; Whitman, L. J. R.; Colton, J. *Biosens. Bioelectron.* **2000**, *14*, 805.

(11) Mannini, M.; Bonacchi, D.; Zobbi, L.; Piras, F. M.; Speets, E. A.; Caneschi, A.; Cornia, A.; Magnani, A.; Ravoo, B. J.; Reinhoudt, D. N.; Sessoli, R.; Gatteschi, D. *Nano Lett.* **2005**, *5*, 1435−1438.

(12) Cavallini, M.; Biscarini, F.; Gómez-Segura, J.; Ruiz, D.; Veciana, J. *Nano Lett.* **2003**, *3*, 1527.

(13) Ruiz-Molina, D.; Mas-Torrent, M.; Gómez, J.; Balana, A. I.; Domingo, N.; Tejada, J.; Martínez, M. T.; Rovira, C.; Veciana, J. *Adv. Mater.* **2003**, *15*, 42.

(14) Blossey, R.; Lorke, A. *Phys. Rev. E* **2002**, *65*, 021603−1.

(15) Lorke, A.; Luyken, R. J.; Garcia, J. M.; Petroff, P. M. *Jpn. J. Appl. Phys.* **2001**, *40*, 1857.

(16) Deegan, R. D.; Bakajin, O.; Dupont, T. F.; Huber, G.; Nagel, S. R.; Witten, T. A. *Nature* **1997**, *389*, 827.

(17) Deegan, R. D.; Bakajin, O.; Dupont, T. F.; Huber, G.; Nagel, S. R.; Witten, T. A. *Phys. Rev. E* **2000**, *62*, 756.

(18) Cordeiro, R. M.; Pakula, T. *J. Phys. Chem. B* **2005**, *109*, 4152.

(19) de Gennes, P.-G.; Brochard-Wyart, F.; Quere, D. *Capillary and wetting phenomena: drops, bubbles, pearls, waves*; Springer: New York, 2004; p 678.

(20) Kim, E.; Xia, Y.; Zhao, X.-M.; Whithesides, G. M. *Adv. Mater.* **1997**, *9*, 651.

(21) Cavallini, M.; Murgia, M.; Biscarini, F. *Nano Lett.* **2001**, *1*, 193.